Polymer 51 (2010) 2077–2083

Contents lists available at ScienceDirect

Polymer

journal homepage: www.elsevier.com/locate/polymer

Carbon black self-networking induced co-continuity of immiscible polymer blends

Guozhang Wu*, Bingpeng Li, Jiandi Jiang

Shanghai Key Laboratory of Advanced Polymeric Materials, School of Materials Science & Engineering, East China University of Science & Technology, Shanghai 200237, PR China

ARTICLE INFO

Article history:
Received 18 November 2009
Received in revised form
27 January 2010
Accepted 2 March 2010
Available online 6 March 2010

Keywords:
Co-continuity
Polymer blends
Carbon black

ABSTRACT

This work aims to clarify the mechanism of nanoparticle-induced co-continuity in immiscible polymer blends. An industrially relevant system, carbon black (CB)-filled acrylonitrile-butadiene-styrene (ABS)/polyamide 6 (PA6) blends, is investigated via scanning electron microscopy, selective extraction tests, dynamic mechanical analysis, and electrical conductivity measurements. The CB particles are found to be preferentially localized in the PA6 phase, and with an increase in CB loading (Φ_{CB}), the critical volume fraction of PA6 (Φ_{PA6}) that is essential for building the co-continuous structure decreases. The product of Φ_{PA6} and Φ_{CB}, n, remains constant for the given system, suggesting that there exists an intrinsic cooperative effect between the CB and the CB-localized polymer phase. A further decrease in Φ_{PA6} is achieved either by loading CB with a higher self-networking capability or by isothermal post-treatments for sufficient self-agglomeration of the CB clusters. It is demonstrated that, under the direction of CB self-networking, the CB-localized polymer domains tend to fuse together into co-continuous organization with little phase coarsening. Therefore, CB self-assembly not only plays a key role in extending phase co-continuity over a much larger composition range but also acts on stabilizing the co-continuous polymer domains during the melt processing.

1. Introduction

The performance of polymer blends is determined not only by the properties of the component polymers, but also by the morphology formed [1–4]. Generally, one polymer is dispersed in another polymer, and the blend forms a sea-island microstructure. As the content of the minor component increases to a critical value, the morphology of polymer blends changes into a co-continuous structure. In recent years, much effort has been devoted to polymer blends with a co-continuous structure due to their substantially improved properties, including elastic modulus, heat resistance, and electrical and thermal conductivity [5–8]. The remaining challenge is how to reduce the critical content of the minor polymer and how to minimize and stabilize the co-continuous polymer domains during the melt processing.

The addition of nanoparticles into immiscible polymer blends has been found effective in extending phase co-continuity over a much larger composition range [8–14]. Gubbels et al. [15] carefully studied the morphology and electrical properties of carbon black (CB)-filled polystyrene (PS)/polyethylene (PE) blends. They found that CB was selectively located in the PE phase, and by adding 4 wt% of CB, the critical PE concentration for maintaining the co-continuous structure was reduced abruptly from 40 wt% to 10 wt%. Li and Shimizu [16] revealed that adding a small amount of nanoclay changes the morphology of polyamide 6 (PA6)/poly(phenylene oxide) (PPO) blends from a sea-island structure to a co-continuous structure. Similar effects were also reported for immiscible polymer blends filled with carbon nanotube [17] or nano-sized silica [18,19].

At present, the underlying mechanism of nanoparticle-induced co-continuity is unclear. According to Paul and Barlow [20], the condition for phase inversion from a sea-island structure to a co-continuous one is expressed as

$$\Phi_1/\Phi_2 = \eta_1/\eta_2 \quad (1)$$

where Φ_i and η_i is the volume fraction and melt viscosity of component i, respectively. That is, an increase in the volume fraction or a decrease in the viscosity of the minor polymer would enhance its continuity in the matrix. The nanoparticle's selective location will indeed give additional volume to the minor polymer. However, in the case of the CB-filled PS/PE system [15], the CB loading is too low (about 4 wt%) to reduce the phase inversion point of PE from 40% to 10 wt%. Furthermore, the selective location of CB will inevitably increase the PE melt viscosity, which will in turn conversely degenerate the co-continuity of the polymer blends according to Eq. (1).

* Corresponding author. Tel./fax: +86 21 64251661.
E-mail address: wgz@ecust.edu.cn (G. Wu).

0032-3861/$ – see front matter © 2010 Elsevier Ltd. All rights reserved.
doi:10.1016/j.polymer.2010.03.007

A good interfacial compatibility between the immiscible polymers may broaden the composition range of co-continuity [1]. Lin et al. [21] demonstrated that nanoparticles could behave like surfactants. Furthermore, Ginzburg [22] and He et al. [23] recently carried out thermodynamic calculations to determine the influence of nanoparticles on the miscibility of homopolymers blends. Both studies found that by decreasing nanoparticle size, a phase-separating system becomes thermodynamically miscible. It should be noted that the nanoparticles used as a compatibilizer in these studies have been carefully modified in order to endow almost the same affinity to both polymers, so that these nanoparticles are preferentially localized at the interface between the immiscible polymers [8]. However, this is not the general case. At least, little evidence supports the improvement of the interfacial compatibility between two immiscible polymers by the aggregated CB clusters.

The most convincing argument at present is that CB increases the viscosity of the CB-localized phase, therefore slowing down the phase coalescence and coarsening process [8,15,17]. It is true that the addition of nanoparticles can reduce the domain size. Furthermore, with an increase in nanoparticle loading, the coarsening of the polymer domains can be suppressed effectively despite a long period of thermal post-treatments above the melting temperature. This leads to a delay in the coarsening-driven break-up of the co-continuous structure. However, new evidence revealed in this work shows an opposite tendency, that is, the degree of co-continuity of the CB-filled immiscible polymer blends increases with an increase in annealing time and temperature. The annealing-induced enhancement of co-continuity is unusual since phase coalescence and coarsening in a binary system are thermodynamically driven by the requirement of minimizing the interfacial free energy.

This work aims to clarify quantitatively the relation between CB loading and the critical concentration of the minor polymer for building the co-continuity, as well as to further elucidate the mechanism of CB-induced co-continuity in immiscible polymer blends. An industrially relevant system, CB-filled acrylonitrile-butadiene-styrene (ABS)/PA6 blends, was studied. ABS consists of a butadiene rubber dispersed in a matrix of styrene-acrylonitrile copolymer, and is generally noted for its excellent toughness, dimensional stability, and relatively low cost. A substantial improvement in the stiffness and heat resistance of ABS/PA6 can be achieved only when the minor PA6 phase is continuous [24]. CB was incorporated not only to serve as a conductive additive but also to act as a modifier to mediate the co-continuity of the ABS/PA6 blends.

2. Experimental section

2.1. Raw materials and sample preparation

ABS (HI-140, LG Chemical) and PA6 (CM1017, Toray) were used in this study. Two kinds of CB, Vulcan XC-72R (Vxc-72R, Cabot) and N326 (Cabot), with different aggregate structures (as listed in Table 1) were selected. ABS/PA6 blends with different compositions were compounded with CB by Haake Rheomixer (Rheotress 600, Haake) at 240 °C and 100 rpm for 10 min. Before mixing, all the resins and CB were dried in a vacuum oven at 80 °C for at least 12 h. The mixtures were compression-molded into sheets with a thickness of about 1.0 mm at 240 °C for 10 min under a pressure of 10 MPa.

2.2. Characterization

Morphology observation was carried out via scanning electron microscope (SEM) (JSM-6360, JEOL) at an accelerating voltage of 15 kV. The specimens were fractured in liquid nitrogen. The fracture surface was then etched using one of the following two methods.

Table 1
Characteristics of CB-filled in polymer blends and the parameter n.

Polymer Blends	Carbon black				n
	Grade name	Diameter (nm)	N_2 Surface Area (m^2/g)	DBP adsorption number (ml/100 g)	
ABS/PA6	N326	30	80	72	98.7
NR/PE[a]	Seast 300	28	86	120	65.6
ABS/PA6	Vxc-72R	30	254	178	45.1
PMMA/PE[b]	VGCF	200	12.5	$L/D = 50$	18.2
PS/PE[c]	Printex XE-2	35	1000	420	9.1

[a] Natural rubber (NR)/PE, data from Ref. [26].
[b] Poly(methyl methacrylate) (PMMA)/PE, data from Ref. [25].
[c] PS/PE, data from Ref. [15].

For the ABS/PA6 blend without CB, formic acid was used as an etching agent to dissolve the PA6 phase; for the CB-filled composite, the surface was etched with tetrahydrofuran (THF) to dissolve the ABS phase. The etched surface was then coated with gold for SEM observation. For polarizing optical microscope (POM, Nikon) observation, thin films about 10 μm in thickness were obtained by compression-molding the mixture at 240 °C for 5 min.

The three-dimensional (3D) co-continuity of the ABS/PA6/CB mixtures in bulk was measured by selective extraction tests. The samples were cut into 10 × 10 × 1 mm^3 sheets and were placed in THF for 3 days at room temperature to extract the ABS phase. As long as the extraction left the sample compact (no fragmentation into smaller pieces), PA6 was considered 100% continuous. In contrast, when the sample fell apart, PA6 continuity was estimated as the weight fraction of the large compact piece of PA6 after extraction over the total weight of PA6 added to the blend.

Dynamic mechanical analysis (DMA) was performed using Rheogel-E-4000 (UBM, Japan) in a stretching mode in order to precisely determine the continuity of PA6 in the ABS matrix. The dynamic storage and loss modulus were measured at a frequency of 10 Hz and a heating rate of 5 °C/min in a temperature range from 0 °C to 250 °C.

CB network formation in the polymer phase was investigated by electrical resistivity measurements. Experiments were carried out in the perpendicular direction of the molded sheets using a Keithley 6487 picoammeter equipped with a direct current voltage source. Silver paste was used to ensure good contact of the sample surface with the copper electrodes. No observable deviation from the four-terminal measurements was found. Thus, DC resistivity in this work was measured using a two-terminal technique. The measurements were carried out at room temperature after stabilizing for 2 min in order to obtain a stationary value.

3. Results and discussion

3.1. Morphology observation

Fig. 1 shows the POM and SEM photographs of the ABS/PA6 blend (80/20, in wt/wt) and its CB-filled composite. The ABS/PA6 blend without CB (Fig. 1a and a') shows typical sea-island morphology, in which PA6 domains several micrometers in size are dispersed in the ABS matrix. PA6 domains were selectively extracted by formic acid in Fig. 1a'. Fig. 1b and b' show the morphology of the ABS/PA6 blend containing 2 phr (per hundred of resin) CB. The dispersed PA6 domains turn black (Fig. 1b), and CB is selectively located in the PA6 phase (Fig. 1b'). The addition of 2 phr CB makes the PA6 domains stick together to some extent in Fig. 1b as compared to that in Fig. 1a.

Fig. 2a and b show the morphology of the ABS/PA6 blend (80/20) filled with 15 phr CB. The ABS matrix was selectively extracted by

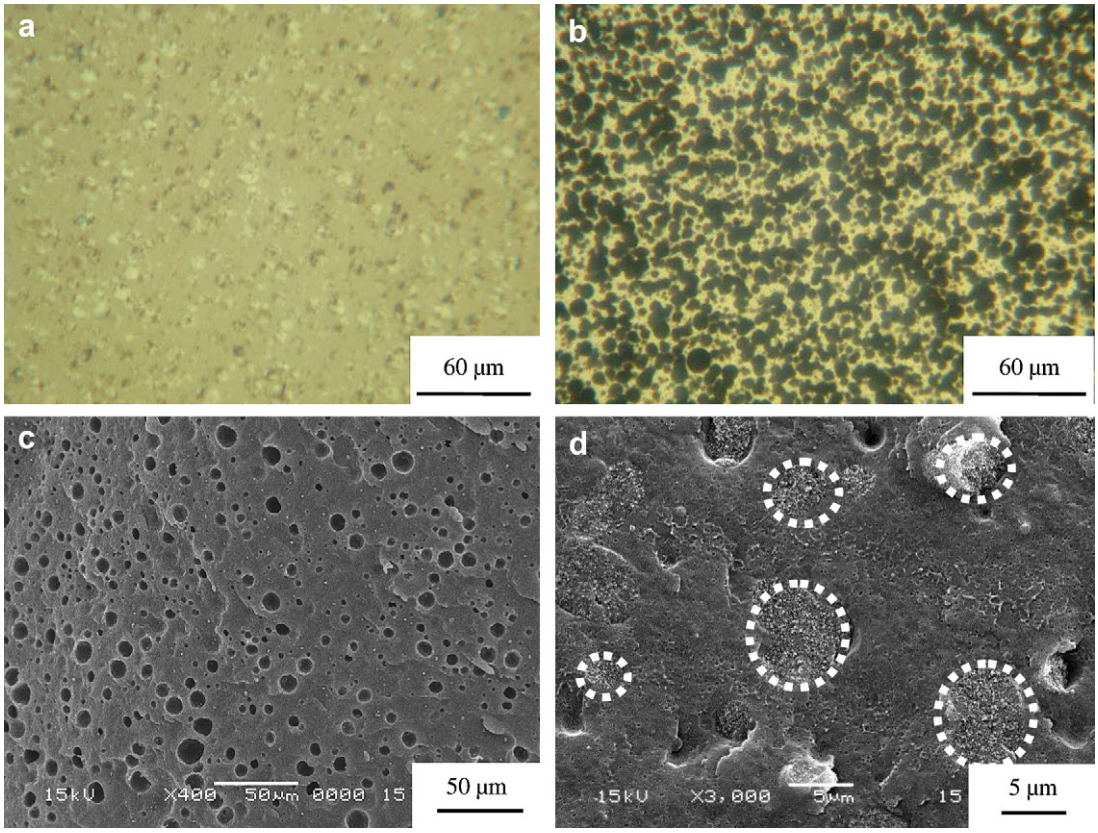

Fig. 1. POM and SEM images of the ABS/PA6 (80/20) blends prepared without CB (a and a') and with 2 phr CB (b and b'). CB is selectively located in PA6 domains as shown by the dashed circle.

THF to clarify the morphology. The sample was observed to have kept its shape even when the ABS matrix was completely dissolved during the extraction process, indicating the formation of self-supported continuous PA6 networks in the ABS matrix. The SEM micrograph at a higher magnification (Fig. 2b) displays the continuous structure of the PA6 phase clearly. Note that CB-localized in the PA6 phase may be covered by PA6 chains during the selective extraction. With an increasing CB content, more and more separate PA6 domains fuse together, and the morphology of the ABS/PA6 blend (80/20) is finally transformed from a sea-island structure into a co-continuous one. A similar transition was also observed in CB-filled ABS/PA6 blends with PA6 content as high as 40 wt% (Fig. 3).

3.2. Degree of co-continuity

Fig. 4 shows the influence of CB loading on the continuity fraction of the PA6 phase for composites with proportions of ABS and PA6 at 60/40, 70/30, and 80/20. Note that these values are estimated by the selective extraction tests. With an increasing CB loading, the continuity fraction of the PA6 phase increases gradually from 0 to 1, demonstrating that the dispersed PA6 domains fuse together to form a completely continuous phase in the ABS matrix. This change should originate from the selective location of CB in the PA6 domains. On the other hand, a higher CB loading is required if the PA6 content is lower. As shown in Fig. 4, for the ABS/PA6 blend with a 60/40 composition, only 2 phr CB is needed to form

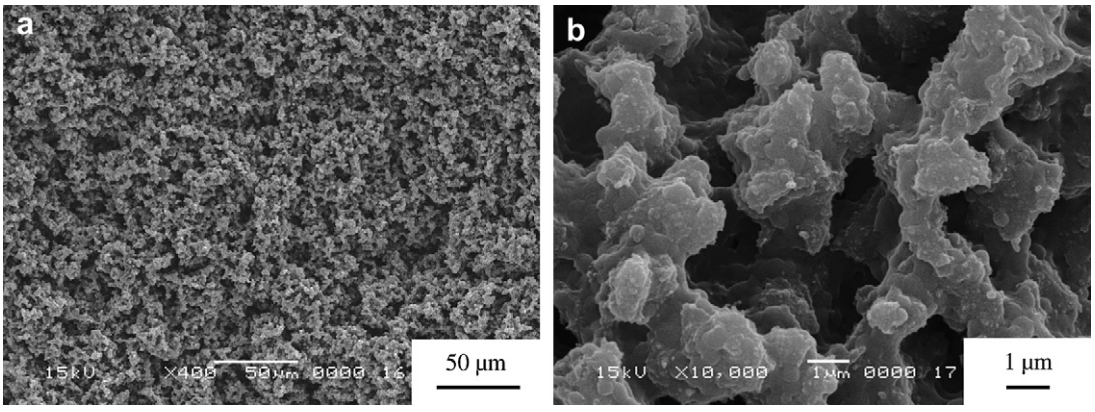

Fig. 2. SEM micrographs of the ABS/PA6 blends (80/20) filled with 15 phr CB. ABS was selectively extracted by THF. (a)×400; (b)×10,000.

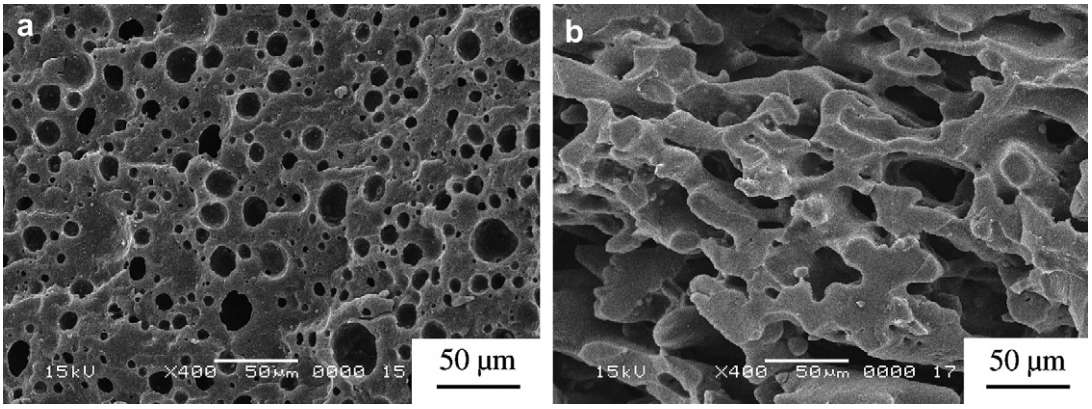

Fig. 3. SEM micrographs of the ABS/PA6 blends (60/40) prepared (a) without CB; PA6 was extracted by formic acid; (b) 7.5 phr CB, ABS was extracted by THF.

a continuous PA6 phase, while for 80/20, the CB content increases to more than 10 phr.

3.3. Dynamic mechanical analysis

To precisely check the continuity of the PA6 phase in the ABS matrix, DMA was carried out for the ABS, PA6, ABS/PA6 blends, and their composites containing various amounts of CB. Fig. 5 shows the temperature dependence of the storage modulus, E′, for ABS, PA6, and their composites filled with 10 phr CB. Obviously, the E′ for PA6 at room temperature is higher than that for ABS. With an increasing temperature, several transitions can be observed. A slight decrease in E′ at about 50 °C corresponds to the glass transition temperature, T_g, of PA6, while the large decrease in E′ at about 106 °C and 220 °C corresponds to T_g of ABS and melting temperature, T_m, of PA6, respectively. The addition of 10 phr CB does not cause a remarkable change in E′ for ABS and PA6.

Due to its high stiffness and heat resistance, PA6 was compounded with ABS to enhance the comprehensive properties. However, as shown in Fig. 6, even the content of PA6 is increased up to 40 wt%, the E′ for the ABS/PA6 blend is almost the same as that for pure ABS in the whole temperature range, indicating that the PA6 domains are separated in the ABS matrix. This is in agreement with SEM observation and selective extraction tests.

A significant change occurs when the ABS/PA6 blend is filled with CB. As shown in Fig. 6a, with the addition of only 2 phr CB, a relatively high E′ remains until the melting temperature of PA6 is reached (about 220 °C), suggesting that the sample should be self-supporting in the high-temperature region. This should be ascribed to the continuity of the PA6 domains in the ABS matrix via the incorporation of 2 phr CB. Although the ABS matrix is very soft and starts to flow in the high-temperature region, the three-dimensional (3D) continuous PA6 phase serves as a mechanical scaffold until it melts above 220 °C. This is consistent with the extraction results shown in Fig. 4. From Fig. 6a, one can also observe that with the increase in CB loadings, the E′ in the high-temperature region increases. The reinforcement should come from either the high strength or the high density of the PA6 networks due to the selective location of more CB particles in PA6 domains.

DMA measurements were systematically carried out for the CB-filled ABS/PA6 blends with various PA6 concentrations. Although the E′ in the high-temperature range decreases with decreasing PA6 content (see Fig. 6b), the morphology transition from a sea-island structure to a co-continuous one is still distinguishable. The transition for ABS/PA6 blends with proportions of 70/30, 80/20, and 90/10 occurs when the CB loading is 3 phr, 5 phr, and 7.5 phr, respectively. It should be noted that these values are lower than those roughly estimated by the selective extraction test because the latter approach cannot detect the weak and brittle PA6 networks.

3.4. A comparison of electrical properties with the DMA results

Fig. 7 shows the dependence of electrical resistivity on the CB loading for the ABS, PA6, and ABS/PA6 blend systems. There is

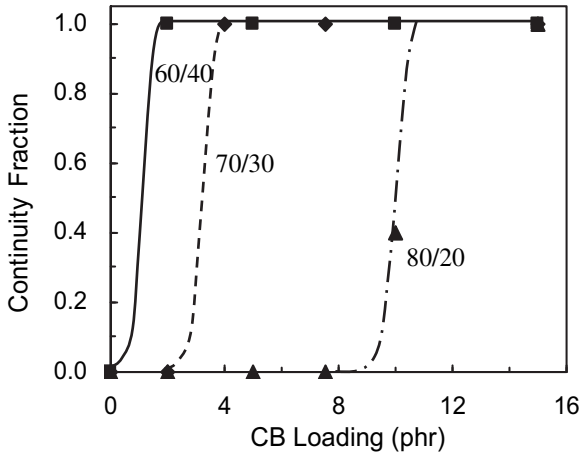

Fig. 4. Dependence of the PA6 continuity fraction on the CB loading with ABS/PA6 at different proportions.

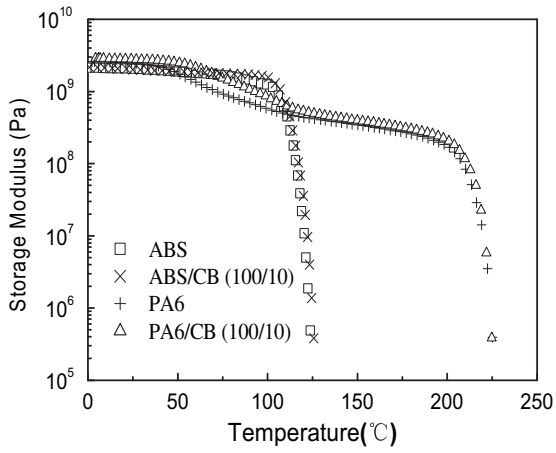

Fig. 5. Temperature dependence of storage modulus for ABS, PA6, and their composites filled with 10 phr CB.

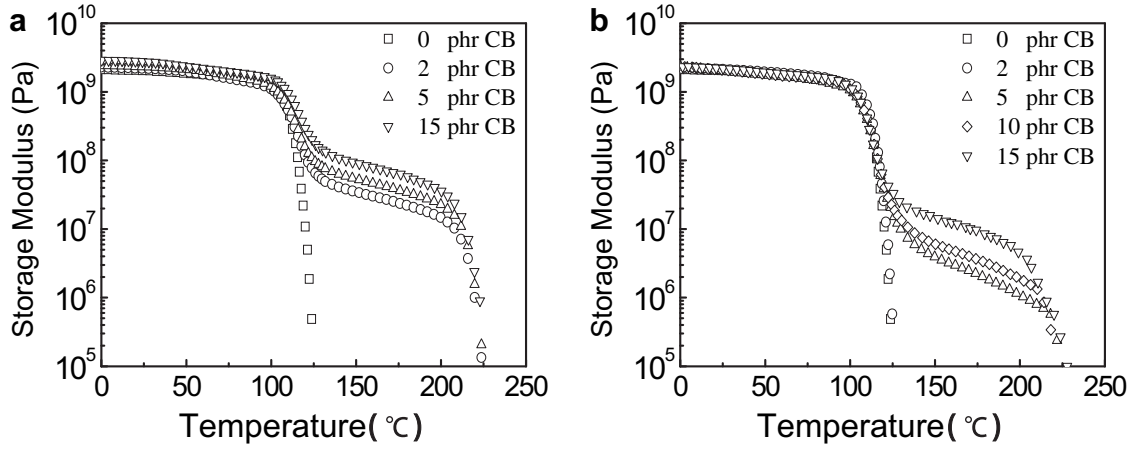

Fig. 6. Temperature dependence of the storage modulus for ABS/PA6 blends containing various amounts of CB. The composition of ABS/PA6 is (a) 60/40; (b) 80/20.

a critical CB loading, called percolation concentration, for each system where the first 3D continuous CB network is built throughout the polymer matrix, and the resistivity of the material begins to decrease abruptly. The percolation concentration in pure ABS and PA6 matrix is observed at 8 phr and 25 phr, respectively. Remarkable improvement in the electrical conductivity of the ABS/CB composites was achieved by adding PA6. As shown in Fig. 7a and b, critical CB loading decreases with the increase in PA6 content. When 40 wt% PA6 is blended with ABS, the percolation concentration can be greatly reduced to 2 phr.

From Fig. 7, the electrical percolation concentration of CB for ABS/PA6 blends with proportions of 90/10, 80/20, 70/30, and 60/40 is 7.5 phr, 4.8 phr, 3.1 phr, and 2 phr, respectively. These values are almost the same as the critical CB loading determined by DMA, at which a mechanical scaffold (which is the continuity of the PA6 phase) forms in the ABS matrix. Since the CB particles are selectively localized in the PA6 domains, the continuity of the PA6 phase is essential for maintaining a conductive network through the composites. It is the double percolation effect that causes the remarkable improvement of electrical conductivity for the ABS/CB composites with addition of PA6. The comparison of electrical properties with the DMA results lets us notice that: (1) measurements of electrical conductivity are effective in checking the co-continuity of the CB-filled immiscible polymer blends; (2) the CB network formation within the PA6 phase may be a prerequisite for driving the minor PA6 phase to fuse together into a continuous structure.

3.5. Correlation of CB loading with critical volume fraction of PA6

Fig. 8 shows a reciprocal plot of PA6 content on critical CB loading for CB (Vxc-72R)-filled ABS/PA6 blends. In the figure, the critical volume fraction of CB, Φ_{CB}, which is the lowest concentration for maintaining the co-continuity of the ABS/PA6 blend at a given volume fraction of PA6, Φ_{PA6}, was determined from the DMA results. It is observed for the first time that the CB-filled system gives a linear plot of Φ_{PA6} vs. $1/\Phi_{CB}$. There exists a quantitative relation between Φ_{CB} and Φ_{PA6} as follows:

$$\Phi_{CB} \times \Phi_{PA6} = n \tag{2}$$

where the parameter n remains constant for the given system. For comparison, another kind of CB (N326) with a different aggregate structure was mixed with the ABS/PA6 blend, and the results are also shown in Fig. 8. Note that all these specimens were prepared under the same procedure and conditions as mentioned above. A linear plot is also obtained though the parameter n increases to a higher value.

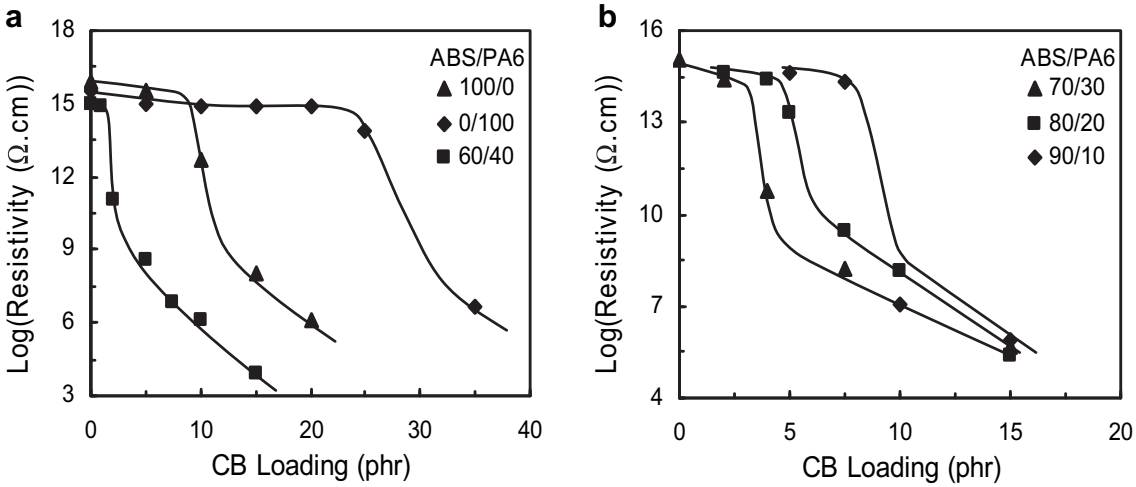

Fig. 7. Resistivity versus CB loadings for (a) the ABS, PA6, ABS/PA6 (60/40), and (b) ABS/PA6 (70/30, 80/20, 90/10) blends.

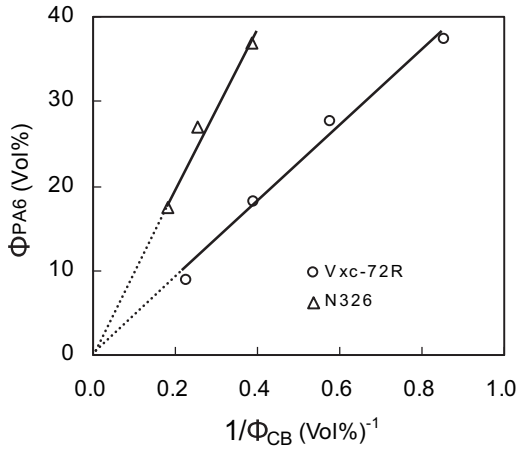

Fig. 8. Reciprocal plots of critical volume fraction of PA6 versus CB loading for CB-filled ABS/PA6 blends.

To confirm the new finding, the reciprocal plots were also performed by rearranging the data previously published by other authors [15,25,26]. In all of those works, PE was the minor phase and the carbon particles were selectively located in the PE phase, despite the fact that the species of carbon particles and matrix polymer were different and were compounded by different conditions. Since the critical loading of carbon particles for electrical percolation has been verified to be almost the same as that from the DMA results, the electrical percolation concentration was used here as Φ_{CB}. As shown in Fig. 9, a family of linear plots between Φ_{PE} and $1/\Phi_{CB}$ is observed. Furthermore, all of the linear plots can be extended to the origin of coordinates, suggesting that there exists an intrinsic cooperative effect between the carbon particle and the carbon-localized polymer phase.

The influence of CB structure on the parameter n in various polymer blend systems is summarized in Table 1. Note that all CB particles have a diameter of about 30 nm. The DBP (*n*-dibutyl phthalate) adsorption number, υ, is a parameter often used for characterizing the CB aggregate structure [27–29]. The vapor-grown carbon fiber (VGCF) listed in Table 1 is a nano-filament, which can be regarded as a CB cluster linearly aggregated with an aspect ratio of about 50 [30]. From Table 1, we find that n decreases with an increase in υ, irrespective of the variety of blend systems. A lower n value means a stronger CB effect on constructing the CB-located polymer's network. Therefore, at a given CB loading, a lower critical volume fraction of the polymer is required by incorporating CB with a higher υ.

Much has been reported [27] that the percolation concentration in the CB-filled polymer composites depends on υ. In a single polymer matrix, Janzen equation [28] has been found adequate to predict the percolation concentration, ϕ_c:

$$\frac{1}{\phi_c} = 1 + \frac{2}{3}C\rho\upsilon \tag{3}$$

where C is the coordination number of nearest neighbors in a specific lattice, ρ the CB density. Eq. (3) shows a decrease of ϕ_c with an increase in υ. This is reasonable because CB with a high υ exhibits a strong self-agglomeration capability to form a CB network in a polymer matrix. Our experimental results listed in Table 1, that is, n decreases with an increase in υ, clearly demonstrates that the self-networking of CB plays a dominant role in the construction of the co-continuous structure in immiscible polymer blends. A relatively low n of the VGCF-filled system can be ascribed to the nano-filament nature of VGCF, which owns a high aspect ratio and favors to form the conductive networks [31].

3.6. Effect of thermal treatment

Our previous studies [31–33] revealed that CB particles are capable of self-assembly in polymer matrices, which can be described in at least two aspects: (1) dynamic percolation and (2) preferential adsorption of polymer chains leading to the selective localization of CB in the polymer blends. CB has a strong tendency to agglomerate in a self-similarity pattern and form 3D conductive networks throughout a matrix. Dynamic percolation occurs [32,33] when the mixture is annealed at temperatures higher than the melting point of the matrix, accompanied by an abrupt reduction of electrical resistivity at a critical annealing time. The percolation time in a single polymer matrix decreases with increasing the annealing temperature. If the continuity of the PA6 phase is driven by the self-networking of CB particles, then the co-continuity in ABS/PA6 blends should be enhanced by annealing at high temperatures.

The effect of thermal treatment on the co-continuity of ABS/PA6 (90/10) filled with 5 phr CB (Vxc-72) was investigated by DMA measurements. As shown in Fig. 10, the storage modulus for the as-produced specimen (hot-pressed at 240 °C for 10 min) drops abruptly and breaks near the T_g of ABS. However, for the specimen that further experienced thermal treatment at 310 °C for 30 min (protected by nitrogen gas), the break point extends to the melting temperature of PA6 at 220 °C, suggesting the existence of continuous PA6 networks through the ABS matrix. This result clearly

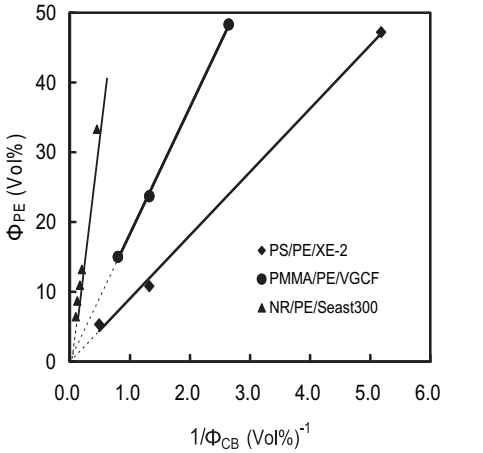

Fig. 9. Reciprocal plots of critical volume fraction of PE versus CB loading for various carbon-filled polymer blends.

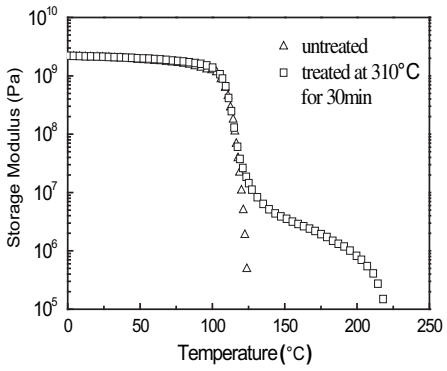

Fig. 10. Temperature dependence of storage modulus for the ABS/PA6/CB (90/10/5) composite.

demonstrated that thermal annealing could give rise to the phase transformation from a sea-island structure to a co-continuous one. Considering that the PA6 chains are preferentially adsorbed on the carbon surface, the annealing-induced enhancement of the co-continuity should arise from the CB self-assembly (i.e., self-networking of the PA6-surrounding CB clusters).

Phase coalescence and coarsening generally take place during the thermal treatment of binary polymer melts due to the requirement of minimizing interfacial free energy. The annealing-induced enhancement of co-continuity in the CB-filled polymer blends appears contrary to the thermodynamic expectation. A reasonable explanation is that the dispersed PA6 domains tend to fuse together in order to minimize the interface area; however, the coarsening of the domain size is greatly suppressed because all of the fused PA6 domains participate in the co-continuous organization under the driving force of the CB self-networking among the PA6 domains. We indeed observed the little change in PA6 domain size for the ABS/PA6 composites highly filled with CB during the thermal annealing. Actually, this phenomenon has already been noticed by Gubbels et al. [15]. They observed a large reduction in the specific interface area of the CB-filled PS/PE blends, while the average size of the phases remains constant with an increasing annealing time. Therefore, CB self-assembly not only plays a key role in extending phase co-continuity over a much larger composition range but also acts on stabilizing the co-continuous polymer domains during the melt processing.

4. Conclusions

Effect of CB on the morphology of ABS/PA6 blends was studied. It was found that CB particles were selectively located in the PA6 phase. The addition of CB leads to a phase transition from a sea-island structure to a co-continuous one. With an increase in CB loading (Φ_{CB}), the PA6 content (Φ_{PA6}) required for the formation of the co-continuous structure decreases. Further experimental results verified that the formation of co-continuity in the immiscible blends was driven by an intrinsic cooperation effect between the CB and the CB-localized PA6 phase. The self-networking of CB plays a key role in extending the phase co-continuity over a much larger composition range.

There exists a quantitative relation between Φ_{CB} and Φ_{PA6}. The product of Φ_{PA6} and Φ_{CB}, n, remains constant for a given system, and decreases with an increase in the DBP adsorption number of CB. This relation appears universal for nanoparticle-filled immiscible polymer blends and may be practically used as guide for designing and controlling their co-continuous morphologies.

The CB self-assembly induced co-continuous structure could significantly improve the mechanical properties of ABS/PA6 blends in the high-temperature range, providing an important approach to fabricate a polymer blend with a desired heat resistance. Meanwhile, due to the heterogeneous distribution of CB and the double percolation effect, the electrical percolation concentration decreased remarkably. Therefore, CB can be regarded as a conductive filler and as a modifier to mediate the morphology of immiscible polymer blends in order to endow composites with multiple high performances.

Acknowledgement

This research was supported by grants from the National Natural Science Foundation of China (50873033, 20974033).

References

[1] Pernot H, Baumert M, Court F, Leibler L. Nat Mater 2002;1(1):54–8.
[2] Baker WE, Scott CE, Hu GH. Reactive polymer blending. Munich: Hanser; 2001 [p. 207–53].
[3] Taguet A, Huneault MA, Favis BD. Polymer 2009;50(24):5733–43.
[4] Chen XH, Ma GQ, Li JQ, Jiang SC, Yuan XB, Sheng J. Polymer 2009;50 (14):3347–60.
[5] Roy X, Sarazin P, Favis BD. Adv Mater 2006;18(8):1015–9.
[6] Li JM, Ma PL, Favis BD. Macromolecules 2002;35(6):2005–16.
[7] Babinec SJ, Mussell RD, Lundgard RL, Cieslinski R. Adv Mater 2000;12(23): 1823–34.
[8] Balazs AC, Emrick T, Russell TP. Science 2006;314(5802):1107–10.
[9] Hom S, Bhattacharyya AR, Khare RA, Kulkarni AR, Saroop M, Biswas A. J Appl Polym Sci 2009;112(2):998–1004.
[10] Al-Saleh MH, Sundararaj U. Compos Part A Appl Sci Manuf 2008;39(2): 284–93.
[11] Kelnar I, Rotrekl J, Kotek J, Kaprálková L. Polym Int 2008;57(11):1281–6.
[12] Wu D, Wu L, Zhang M, Zhou W, Zhang Y. J Polym Sci Part B Polym Phys 2008;46(12):1265–79.
[13] Filippone G, Dintcheva NT, Acierno D, La Mantia FP. Polymer 2008;49(5): 1312–22.
[14] Wu D, Zhou C, Zhang M. J Appl Polym Sci 2006;102(4):3628–33.
[15] Gubbels F, Blacher S, Vanlathem E, Jérôme R, Deltour R, Brouers F, et al. Macromolecules 1995;28(5):1559–66.
[16] Li YJ, Shimizu H. Polymer 2004;45(22):7381–8.
[17] Zou H, Wang K, Zhang Q, Fu Q. Polymer 2006;47(22):7821–6.
[18] Steinmann S, Gronski W, Friedrich C. Polymer 2002;43(16):4467–77.
[19] Liu W, Huang Y, Wu D, Gao L, Yang Q, Li G. Acta Polym Sin 2009;6:553–9.
[20] Paul DR, Barlow JW. J Macromol Sci Rev Macromol Chem 1980;C18(1):109–68.
[21] Lin Y, Skaff H, Emrick T, Dinsmore AD, Russell TP. Science 2003;299 (5604):226–9.
[22] Ginzburg VV. Macromolecules 2005;38(6):2362–7.
[23] He G, Ginzburg VV, Balazs AC. J Polymer Sci Pt B Polymer Phys 2006;44 (17):2389–403.
[24] Kudva RA, Keskkula H, Paul DR. Polymer 2000;41(1):225–37.
[25] Zhang C, Yi XS, Asai S, Sumita M. Compos Interfac 1999;6(4):287–96.
[26] Wu G. Design and control of carbon black networks in polymer composites: thermodynamics, kinetics and characterization. Tokyo Institute of Technology, PhD thesis; 2000.
[27] Donnet J-B, Voet A. Carbon black: physics, chemistry, and elastomer reinforcement. New York: Marcel Dekker; 1976 [p. 211–23].
[28] Janzen J. J Appl Phys 1975;46(2):966–9.
[29] Kraus G, Svetlik JF. J Electrochem Soc 1956;103(6):337–42.
[30] Wu G, Asai S, Sumita M, Hattori T, Higuchi R, Washiyama J. Colloid Polym Sci 2000;278(3):220–8.
[31] Wu G, Asai S, Sumita M, Yui H. Macromolecules 2002;35(3):945–51.
[32] Wu G, Asai S, Zhang C, Miura T, Sumita M. J Appl Phys 2000;88(3):1480–7.
[33] Wu G, Asai S, Sumita M. Macromolecules 2002;35(5):1708–13.